



# Synthesis and Characterization of Titanium Dioxide Films and There Application In P3HT/TiO<sub>2</sub> Hybrid Solar Cells

## KEYWORDS

Nanocrystalline TiO<sub>2</sub>, Sol-Gel, AFM, XRD, Solar cells

**Haidar Gazy Lazim**

Department of Science. College of Basic Education, Misan University

**Khalid. I. Ajeel**

Department of Physics, College of Education for Pure Science, Basrah University

**Aseel Hassan**

Materials and Engineering Research Institute, Sheffield Hallam University, Sheffield, UK

**ABSTRACT** In this work, p-type poly (3-hexylthiophene-2,5-diyl) (P3HT) and n-type nano-anatase titanium dioxide (TiO<sub>2</sub>) structure have been various photovoltaic (PV) devices onto indium tin oxide (ITO) coated glass substrates and silicon. These films were deposited by spin coating at 2000 rpm. X-ray diffraction (XRD) patterns confirmed that polycrystalline TiO<sub>2</sub> anatase phase formation. The optical properties of Solar Cell under the effect of the light equivalent to that of the sun radiation on the sample were studied. The highest Voc and power conversion efficiency were 0.45V and 0.23% fabricated with 550  $\mu$ C respectively.

## 1. Introduction

Organic solar cells have attracted great attention due to the advantages of light weight, flexibility and low cost with the possibility of fabricating large area device by cheaper liquid based process. However, the power conversion of organic solar cells is limited by the low dissociation probability of excitons and inefficient hopping carrier transport [1]. Therefore, improving the performance of the solar cells has been resolved in building bilayer and bulk heterojunction structure with phase separation between the polymer and inorganic nano materials, such as TiO<sub>2</sub> nanocrystals. Titanium dioxide (TiO<sub>2</sub>) has attracted considerable attention for its potential applications in optical components including solar cell, photocatalysis, chemical sensors, and optical filters [2-5].

The material can be formulated as nano films by using a variety of techniques such as pulsed laser deposition (PLD) [6-8], chemical vapour deposition (CVD) [9-10], and sol-gel coating [11-12]. TiO<sub>2</sub> has three main crystal phases (anatase, rutile, and brookite). Among these phases, anatase phase, which is a meta-stable phase, is also chemically and optically active and suitable for photocatalyst [13]. In dye-sensitized solar cells, photoelectrodes prepared using anatase phase TiO<sub>2</sub> gives better solar cell efficiency compared to the other crystal structures. Optical properties of TiO<sub>2</sub> include a wide band gap, high transparency in the visible spectrum and a high refractive index over a wide spectral range (from ultraviolet (UV) to the far infrared (IR)). Nanocrystalline titanium TiO<sub>2</sub> is also a promising semiconductor for applications based on its photoconductivity. The reported optical gap of TiO<sub>2</sub> is in the range of 3-3.7 eV corresponding to the ultraviolet region of the solar spectrum [14].

In the present study we report on the synthesis and characterization of nanocrystalline TiO<sub>2</sub> and influences of heat treatment on structural and electronic transition of nanocrystalline titanium dioxide films prepared by sol-gel spin coating. It can be shown, that these films are suitable for applications in polymer optoelectronic devices. One of the most important techniques is spectroscopic ellipsometry, which has been found favourably for non-destructive, characterization of thin solid films and bulk materials, especially semiconductors. This technique is of high sensitivity, high accuracy, of being able to easily in situ measure both optical constant and thickness simultaneously [15].

## 2. Experimental

Nanocrystalline like structured TiO<sub>2</sub> films have been prepared by sol-gel spin coating method using a standard photoresist spinner (Model 4000 Electronic Micro System). The gel was spin coated on Si and a cleaned ITO-glass substrates at 2000 rpm for nano films of TiO<sub>2</sub> prepared from Titanium Isopropoxide (TIP) of chemical construction (C<sub>12</sub>H<sub>28</sub>O<sub>4</sub>Ti) of purity (99.99%), also from (Acetic Acid) (CH<sub>3</sub>COOH) of purity (99.5%), and also from (Ethanol) (C<sub>2</sub>H<sub>5</sub>OH) with purity of (99.7%). These materials were prepared of (Aldrich Chemicals Company). These films have been characterized by XRD, and Spectroscopic Ellipsometry were investigated on TiO<sub>2</sub> films spin coated onto silicon substrates using a Woolam M-2000V that rotated compensator spectroscopic Ellipsometry in the wavelength of range from 370-1000 nm. The fixed degree of the angle of incidence was 70°. The thickness of the TiO<sub>2</sub> film and P3HT were found to be approximately 70 nm and 95 nm respectively. The surface morphology was examined by atomic force microscopy (AFM-Digital Instruments Nano Scope). The optical absorbance and transmittance measurements were made on TiO<sub>2</sub> nano films by UV-VIS spectrophotometer at a normal incident of light in the wavelength range of 320-900 nm. After coating, the sol-coated glass substrate was immediately placed in a preheated oven. A furnace type, (CAUTION) was used in this work which has a temperature range of (25-1000 °C). A solution of the p-type organic semiconductor P3HT (Aldrich) in chloroform (20 mg ml<sup>-1</sup>) was prepared by spin coating method at 1500 rpm. The device was completed by evaporating a 4x5 matrix of 60 nm thick, circular gold electrodes onto the P3HT. Chemical formula of P3HT and schematic demonstration of (ITO/TiO<sub>2</sub>/P3HT/Au) are given in Fig. (1).

I-V measurement is used to obtain information on the photovoltaic and electrical properties of the fully fabricated devices. A Keithly 280 programmable voltage source and a Keithly 619 Electrometer/ Multimeter were used for I-V measurements. It is contained in a box and has a solar simulator in which solar cell I-V characteristics were obtained. A 250 W tungsten-halogen source was illuminated and adjusted to give 100 mW cm<sup>-2</sup>. A standard Si-solar cell was used as a reference for calibration. A general purpose interface board (GPIB) link attached to the system which was under computer control collected and stored the relevant I-V characteristics automatically.

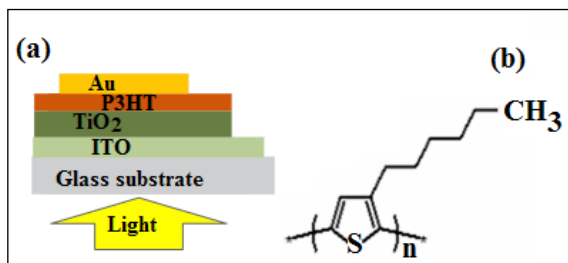


**Figure 1 : schematic demonstration of (ITO/TiO<sub>2</sub>/P3HT/Au) bilayer PVdevice (a) and Chemical formula of P3HT (b).**

### 3. Results and Discussion

X-ray diffraction patterns of the TiO<sub>2</sub> nano films have been shown in Fig. (2) at temperature 550°C. It is obvious that the film is polycrystalline. The structure of TiO<sub>2</sub> in XRD investigation is anatase titanium dioxide, which agrees with (ASTM data 01-071-1166) card [16].

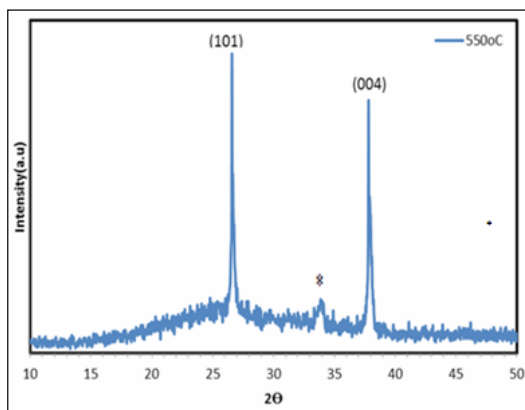


**Figure 2 : XRD patterns of TiO<sub>2</sub> films grown on ITO- glass substrates at heat treatment temperature 550°C(\* for substrate).**

Fig. (3-5) shows AFM images of the pure nanoanatase TiO<sub>2</sub> films heated at different temperatures. We observed that the particle size increased with the increasing heat treatment temperature. The RMS surface roughness of the nanoanatase TiO<sub>2</sub> films was determined to be (0.161, 0.223, 0.552, 0.810 and 1.494 nm) and the particles size are found to be (2.184, 2.378, 4.534, 5.125 and 8.336 nm) for the 250, 350, 450, 550 and 650 °C heat treatment temperature values respectively.

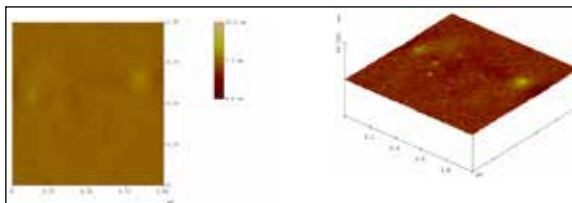


**Figure 3 : Two and three-dimensional AFM images of TiO<sub>2</sub> films at heat treatment temperature 250°C.**

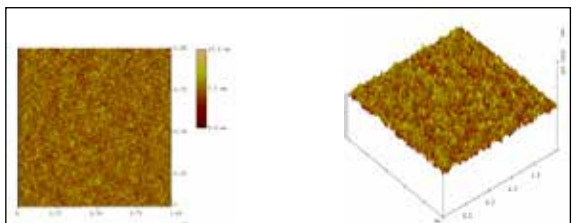


**Figure 4 : Two and three-dimensional AFM images of TiO<sub>2</sub> films at heat treatment temperature 550°C.**

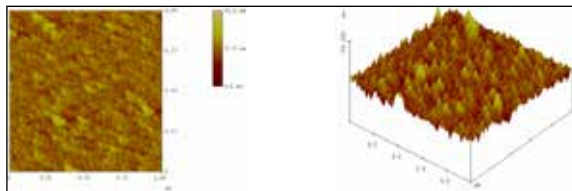


**Figure 5 : Two and three-dimensional AFM images of TiO<sub>2</sub> films at heat treatment temperature 650°C**

Absorption spectra of pure nanoanatase TiO<sub>2</sub> films were analysed using a UV-VIS spectrophotometer, as shown in Fig. (6). When the heat treatment temperature of the films increased, the absorbance is also increased.

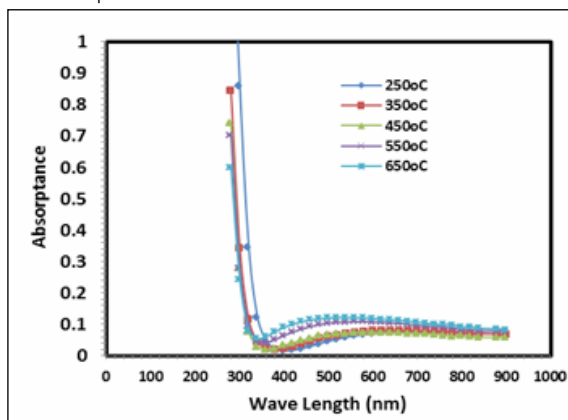


**Figure 6 : Absorption spectra of TiO<sub>2</sub> films with different heat treatment heat treatment.**

Absorption spectra of pure P3HT films were analysed using a UV-VIS spectrophotometer, as shown in Fig. (7).

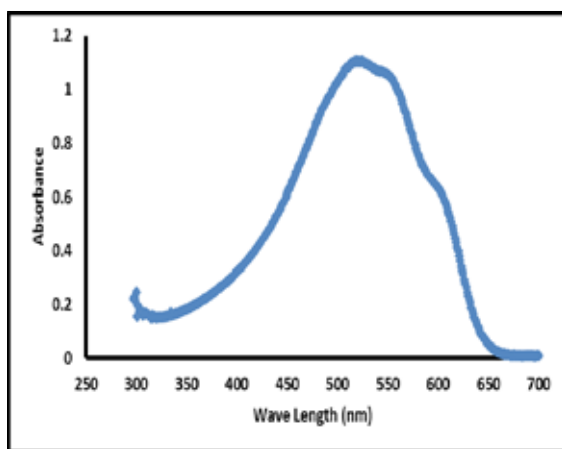


**Figure 7: Absorption spectra of P3HT films**

The uv-vis spectrophotometer of P3HT film absorbs from about 350 nm to 650 nm, thus the TiO<sub>2</sub>

layer has the potential to extend the spectral response of P3HT-based solar cells. Moreover, the

TiO<sub>2</sub> layer can protect the polymer over layer from photo-bleaching by absorbing UV light.

The band gap energy calculated by Spectrophotometric data using following equation [17].

$$ah\nu = B(h\nu - E_g)^n \dots\dots\dots (1)$$

where  $\alpha$  is the absorption coefficient,  $h\nu$  is the photon en-

ergy in eV,  $E_g$  is the band gap energy in eV, B is constant depended on type of material,  $n = 1/2$  for the allowed direct transition.  $n = 3/2$  for the forbidden direct transition. The relations are drawn between  $(\alpha h\nu)^2$ ,  $(\alpha h\nu)^{2/3}$  and photon energy ( $h\nu$ ) as shown in Fig.(8) which illustrates allowed direct electronic transition and Fig.(9) illustrates the forbidden direct electronic transition.

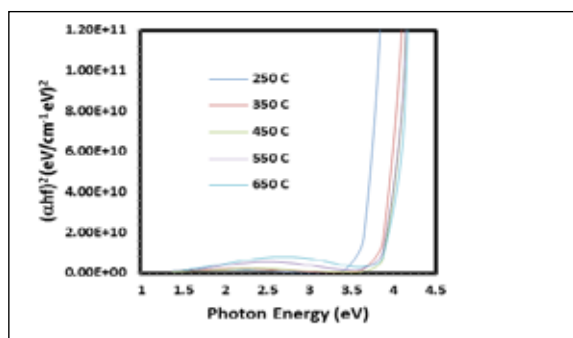


Figure 8:  $(\alpha h\nu)^2$ - $h\nu$  graphs of nanoanatase  $\text{TiO}_2$  films for different heat treatment temperature.

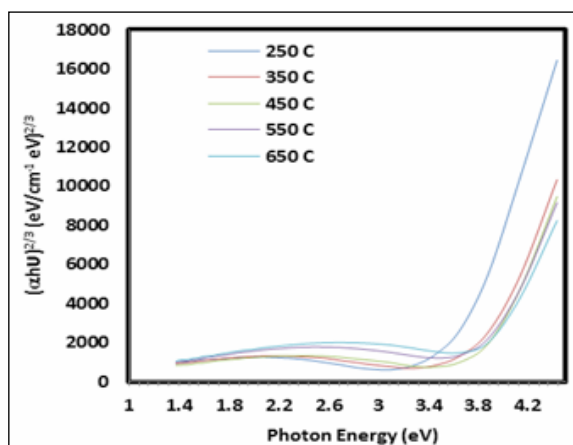


Figure 9 :  $(\alpha h\nu)^{2/3}$ - $h\nu$  graphs of nanoanatase  $\text{TiO}_2$  films for different heat treatment temperature.

The obtained band gap values are given in table (1). This result is in good agreement with earlier studies in which a direct optical transition was reported in the range 3.3-3.79 eV [18-19].

Table 1: direct energy gap for allowed and forbidden direct transition for nanoanatase  $\text{TiO}_2$  films.

Temperature (°C)	Allowed direct transition $E_g(A)(\text{eV})$	Forbidden direct transition $E_g(F)(\text{eV})$
250	3.45	3.28
350	3.62	3.39
450	3.68	3.6
550	3.69	3.61
650	3.75	3.62

The band gap energy of  $\text{TiO}_2$  films changed with different particle size, as seen in the AFM results. We observed that the particle size of pure nanoanatase  $\text{TiO}_2$  films increased with increasing band gap energy, as shown in Fig. (10).

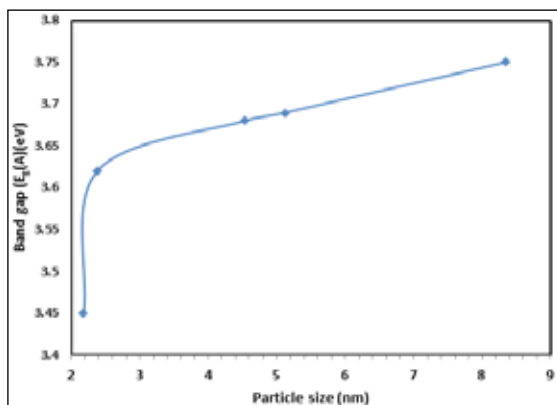


Figure 10. Band gap energy-particle size graphs of nanoanatase  $\text{TiO}_2$  films for different heat treatment temperature.

The energy conversion efficiency ( $\eta$ ) can be determined by the following equation [20]:

$$\eta = \frac{\text{Output Power}}{\text{Input Power}} \times 100\% = \frac{P_{out}}{P_{in}} \times 100\% \quad \dots\dots\dots(2)$$

when ( $P_{in} = 100 \text{ mW/cm}^2$ ) is taken as the solar power incident on a unit area, the ratio between

$(I_p V_p / I_{sc} V_{oc})$  called Fill Factor (F.F.) is a measure power that can get it from solar cell. It can be

written in the following form when the current ( $I_p$ ) replaced by current density ( $J_{sc}$ ).

$$F.F. = (J_p V_p) / (J_{sc} V_{oc}) \quad \dots\dots\dots(3)$$

where  $J_p$  is the maximum current density,  $J_{sc}$  is the Short Circuit Current density,  $V_p$  is the maximum voltage and  $V_{oc}$  is the Open Circuit voltage. Thus [21]:

$$\eta(\%) = ((V_{oc} J_{sc} F.F.) / P_{in}) \times 100 \quad \dots\dots\dots(4)$$

Solar cells are made of P3HT which put on  $\text{TiO}_2$  at different heat treatment temperature. Figures (11- 15) shows the relationship between current and voltage in light and dark of photovoltaic devices based on configuration of type  $\text{ITO}/\text{TiO}_2/\text{P3HT}/\text{Au}$  under  $100 \text{ mW/cm}^2$  and the relevant parameters were summarized in Table (2).

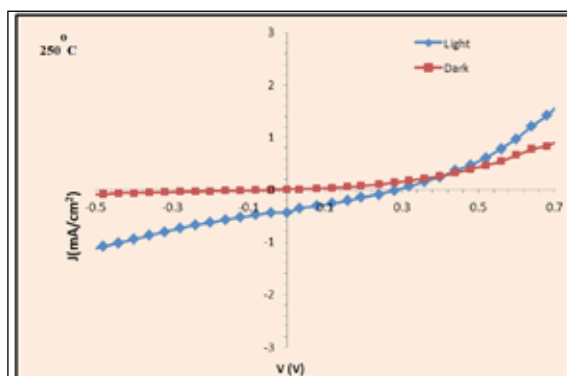


Figure 11: Current density-voltage of the Photovoltaic cell for  $\text{TiO}_2(250^\circ\text{C})/\text{P3HT}$ .

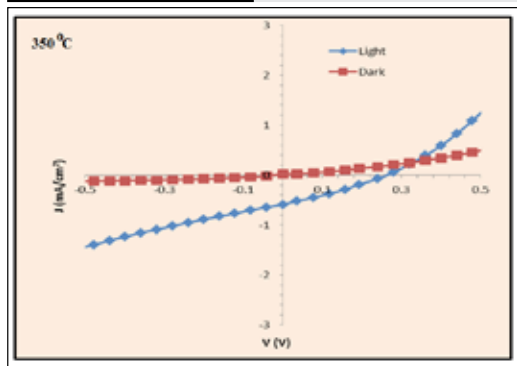


Figure 12 : Current density-voltage of the Photovoltaic cell for  $\text{TiO}_2$  (350°C)/P3HT.

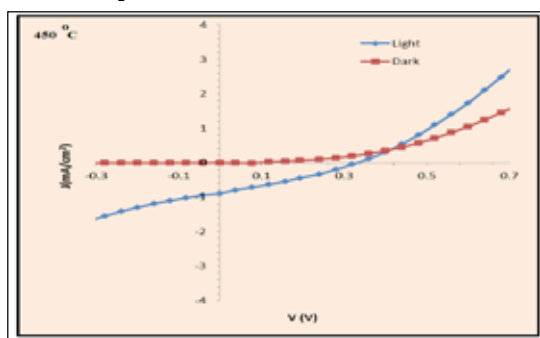


Figure 13 : Current density-voltage of the Photovoltaic cell for  $\text{TiO}_2$  (450°C)/P3HT.

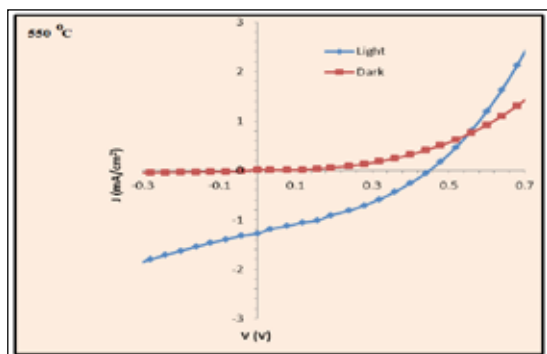


Figure 14 : Current density-voltage of the Photovoltaic cell for  $\text{TiO}_2$  (550°C)/P3HT.

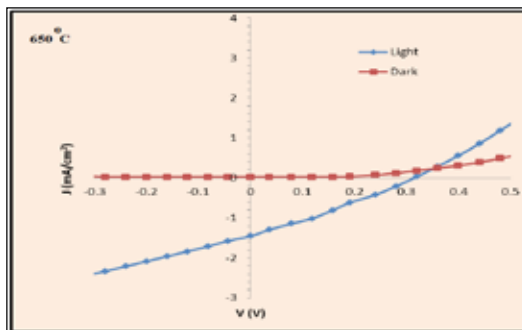


Figure 15 : Current density-voltage of the Photovoltaic cell for  $\text{TiO}_2$  (650°C)/P3HT.

Table (2) The parameter obtained from the (J-V) characteristic of (different heat treatment temperature  $\text{TiO}_2$ /P3HT) solar cell.

Temperature T (°C)	$V_{oc}$ (volt)	$J_{sc}$ (mA/cm <sup>2</sup> )	$V_p$ (Volt)	$J_p$ (mA/cm <sup>2</sup> )	$P_{max}$ (mW/cm <sup>2</sup> )	FF	Efficiency (%)
250	0.29	0.44	0.078	0.38	29	0.23	0.029
350	0.25	0.58	0.118	0.37	43.6	0.3	0.043
450	0.35	0.87	0.158	0.54	85.3	0.28	0.085
550	0.45	1.28	0.28	0.85	238	0.39	0.23
650	0.32	1.46	0.173	0.81	140	0.3	0.14

#### 4. Conclusion

In this study, it can be withdrawn the following conclusions, Titanium dioxide films were prepared through a sol-gel process. The investigation of XRD indicates that the  $\text{TiO}_2$  film is polycrystalline type of anatase. It was found that the particle size controlled by the heat treatment temperature. The results indicate that an increase in the heat treatment temperature led to the increase in the particle size of  $\text{TiO}_2$  films because of the increasing crystallization. The roughness of pure nanoanatase  $\text{TiO}_2$  films increased with increasing particle size. The optical absorbance of nanoanatase  $\text{TiO}_2$  film increased with increased heat treatment temperature. The optical band gap of the films has been found to be in the range 3.28-3.62 eV for the forbidden direct electronic transition and 3.45-3.75 eV for the allowed direct transition for the different heat treatment. The highest  $V_{oc}$  and power conversion efficiency were found to be 0.45V and 0.23% fabricated with 550°C respectively. These results show that it is possible to apply  $\text{TiO}_2$  films to the fabricate of low cost organic devices.

#### REFERENCE

- [1] Kuo CY, Tang WC, Gau C and Jeng DZ (2008). Ordered bulk heterojunction solar cells with vertically aligned  $\text{TiO}_2$  nanorods embedded in a conjugated polymer, *Applied Physics Letters*. 471 033307-1. || [2] Gamez F, Reyes A, Hurtado P, Guille E, Anta JA, Martez B (2010) Nanoparticle  $\text{TiO}_2$  Films Prepared by Pulsed Laser Deposition: Laser Desorption and Cationization of Model Adsorbents, *J. Phys. Chem. C* 114 17409. || [3] Ayeko1 C, Musembi R, Waita1 S, Aduda1 B, P. Jain (2010). Structural and Optical Characterization of Nitrogen-doped  $\text{TiO}_2$  Thin Films Deposited by Spray Pyrolysis on Fluorine Doped Tin Oxide (FTO) Coated Glass Slides, *International Journal of Energy Engineering*. 2 67. || [4] Mohammadi M, Shahtahmaseb N, Karimipour1 M, Sarhadd R (2012). Characterization of nanostructured Nd-doped  $\text{TiO}_2$  thin film synthesized by spray pyrolysis method: Structural, optical and magneto-optical properties, *Indian Journal of Science and Technology*. 5 2912. || [5] Ayicko C, Musembi R, Waita S, Jain P (2012). Structural and Optical Characterization of Nitrogen-doped  $\text{TiO}_2$  Thin Films Deposited by Spray Pyrolysis on Fluorine Doped Tin Oxide (FTO) Coated Glass Slides, *International Journal of Energy Engineering*. 2 67. || [6] Han X, Wang G, Jie J, Zhu X, Hou J (2005). Properties of Zn1-xCoxO thin films grown on silicon substrates prepared by pulsed laser deposition, *Thin Solid Films*. 491 249. || [7] Hyuck S, Yeol S, Jun B, Seongil I (2000). Pulsed laser deposition of ZnO thin films for applications of light emission, *Applied Surface Science*. 154 458. || [8] Singh A, Kumar M, Mehra R, Wakahara A, Yoshida A (2001). Al-doped zinc oxide (ZnO:Al) thin films by pulsed laser ablation, *J. Indian Inst.* 81 527. || [9] Capan R, Chaur N, Hassan A (2004). Optical dispersion nanocrystalline titanium thin films, *Semiconductor Science and Technology*. 19 198. || [10] Rathee D, Kumar M, Arya S (2012). Deposition of nanocrystalline  $\text{TiO}_2$  films for MOS capacitors using Sol-Gel spin method with Pt and Al top electrodes, *Solid-State Electronics*. 76 71. || [11] Ibrahim N, Yusianto E, Ibrahim Z (2012). Effect of Different  $\text{TiO}_2$  Preparation Techniques on the Performance of the Dielectric Bolometer as a Distance Sensor, *Sains Malaysiana*. 41 1092. || [12] Shih H, Vasant R (2012). Sol-gel  $\text{TiO}_2$  in self-organization process: growth, ripening and sintering. *RSC Advances*. 2 2294. || [13] Landmann M, Rauls E, Schmidt W (2012). The electronic structure and optical response of rutile, anatase and brookite  $\text{TiO}_2$ , *J. Phys. Chem. C* 116 2294. || [14] ThiThanh LD, Vuongb D, Duya NV (2009). Preparation and characterization of solid n- $\text{TiO}_2$ /p-NiO heterojunction electrodes for all-solid-state dye-sensitized solar cells, *Solid-State Electronics*. 53 111. || [15] Jiang H, Wei Q, Xiyao Q (2008). Spectroscopic ellipsometry characterization of  $\text{TiO}_2$  thin films prepared by the sol-gel method, *Ceramics International*. 34 1039. || [16] ASTM data (01-071-1166) card. || [17] Singh AP, Kumari S, Shrivastav R (2008). Iron doped nanostructured  $\text{TiO}_2$  for photoelectron-chemical generation of hydrogen, *International Journal of Hydrogen Energy*. 33 5363. || [18] Wang Z, Helmersson U, Kall P (2002). Optical properties of  $\text{TiO}_2$  thin film prepared by aqueous sol-gel at low temperature, *Thin Solid Film*. 405 50. || [19] Lazim HG, Ajeel KI, Hassan AK (2013). Effect of Heat Treatment on Structural and Electronic Transition of Nano-Crystalline Titanium Dioxide Film, *IOSR Journal of Applied Physics*. 3 8. || [20] Kao MC, Chen HZ, Young SL (2011). Dye-sensitized solar cells with  $\text{TiO}_2$  nanocrystalline films prepared by conventional and rapid thermal annealing processes. *Thin Solid Films* 519 3268. || [21] Shengli L, Sam S, Junfeng N (2012). Poly(thienylene methane) grafted nanocrystalline  $\text{TiO}_2$  based hybrid Solar Cell, *J Mater Sci: Mater Electron*. 23 251. ||